A&A 379, 235–244 (2001)
DOI: 10.1051/0004-6361:20011334

Astronomy & Astrophysics

Early type stars at high galactic latitudes

II. Four evolved B-type stars of unusual chemical composition⋆,⋆⋆,⋆⋆⋆

M. Ramspeck, U. Heber, and H. Edelmann

Dr. Remeis-Sternwarte, Universität Erlangen-Nürnberg, Sternwartstr. 7, 96049 Bamberg, Germany

Received 26 July 2001 / Accepted 10 September 2001

Abstract. We present the result of differential spectral analyses of a further four apparently normal B-type stars. Abundance anomalies (e.g. He, C, N enrichment), slow rotation and/or high gravities suggest that the programme stars are evolved low-mass B-type stars. In order to trace their evolutionary status several scenarios are discussed. Post-AGB evolution can be ruled out. PG 0229+064 and PG 1400+389 could be horizontal branch (HB) stars, while HD 76431 and SB 939 have already evolved away from the extreme HB (EHB). The low helium abundance of HD 76431 is consistent with post-EHB evolution. The enrichment in helium, carbon and nitrogen can be explained either by deep mixing of nuclearly processed material to the surface or by diffusion processes modified by magnetic fields and/or stellar winds. A kinematic study of their galactic orbits indicates that the stars belong to an old disk population.

Key words. Galaxy: halo – stars: early-type – stars: abundances – stars: kinematics – stars: evolution

1. Introduction

The population of faint blue stars at high galactic latitudes is dominated by subluminous O- and B-type stars. However, several objects among the faint blue stars are apparently normal B-type stars because their spectra closely resemble that of main sequence stars (see Tobin 1987; Keenan 1992; Heber et al. 1997 for reviews).

Tobin (1987) discusses the problem that some highly evolved stars spectroscopically mimic normal massive stars almost perfectly. The most striking example is PG 0832+676 which has been analysed several times. Its abundance pattern is close to normal. Only recently, Hambly et al. (1996) were able to firmly establish slight underabundances and a very low projected rotation velocity. Combining both results they concluded that PG 0832+676 in fact is a highly evolved star. In a recent paper, Hambly et al. (1997) extended their study to a dozen apparently normal B-type stars and demonstrated that they are also of low-mass.

Abundance analyses as well as determinations of rotational velocities are thus essential to distinguish massive from low-mass stars. A high rotational velocity generally excludes a late evolutionary status of the star, as old, low-mass stars cannot rotate as fast as massive stars.

During our ongoing investigation of faint blue stars we encountered several apparently normal B-type stars (Moehler et al. 1994; Heber et al. 1995; Schmidt et al. 1996). In a recent paper we described the spectral analysis of ten massive B-type stars at high galactic latitudes (Ramspeck et al. 2001, henceforth Paper I).

Here we present the analysis of new high-resolution spectra for four additional stars which were classified as apparently normal from spectra of lower spectral resolution. We have obtained high resolution Echelle spectra for PG 0229+064, PG 1400+389, HD 76431 and SB 939 using the HIRES spectrograph at the Keck I telescope, the FOCES spectrograph at the DSAZ 2.2 m telescope and the CASPEC spectrograph at the ESO 3.6 m telescope. The data set is supplemented by long slit spectra obtained at the DSAZ 3.5 m telescope and the ESO 1.5 m telescope. Details of the observations are given in Table 1 and the data reduction technique is outlined in Paper I.

The atmospheric parameters, rotational velocities and metal abundances are determined in Sects. 2 and 3.

Send offprint requests to: M. Ramspeck,
e-mail: ramspeck@sternwarte.uni-erlangen.de

⋆ Based on observations obtained at the W. M. Keck Observatory, which is operated by the Californian Association for Research in Astronomy for the California Institute of Technology and the University of California.

⋆⋆ Based on observations collected at the German-Spanish Astronomical Center (DSAZ), Calar Alto, operated by the Max-Planck-Institut für Astronomie Heidelberg jointly with the Spanish National Commission for Astronomy.

⋆⋆⋆ Based on observations collected at the European Southern Observatory (ESO proposal No. 65.H-0341(A)).

Table 1. Observational details.

Name	Obs. date	Tel. & Instrum.	$\Delta\lambda$ (nm)
	Echelle spectra		
PG 0229+064	Jul. 20, 1998 14:37	K+H	360–513
	Sep. 13, 1998 03:00	CA+F	387–683
PG 1400+389	Jul. 23, 1996 20:00	K+H	426–670
HD 76431	Feb. 01, 2000 02:00	CA+F	389–693
SB 939	Oct. 1986	E+C	406–513
	Long slit spectra		
PG 0229+064	Nov. 21, 1988 04:39	E+B&C	403–491
PG 1400+389	Apr. 14, 2001 00:28	CA+T	410–495
HD 76431	Apr. 13, 2001 20:53	CA+T	410–495

K+H: KECK I + HIRES (spectral resolution: 0.09 Å).
CA+F: Calar Alto 2.2 m + FOCES (sp. resolution: 0.15 Å).
E+C: ESO 3.6 m + CASPEC (sp. resolution: 0.2 Å).
E+B&C: ESO 1.5 m + B&C (sp. resolution: 2.5 Å).
CA+T: Calar Alto 3.5 m + Twin (sp. resolution: 1.0 Å).

Then the evolutionary status (Sect. 4) and the kinematics of the stars (Sect. 5) are discussed. The last section summarizes the conclusions.

2. Atmospheric parameters and rotational velocities

Effective temperatures, surface gravities and photospheric helium abundances are derived by matching the Balmer and helium line profiles to a grid of synthetic spectra calculated from LTE model atmospheres as described in detail in Paper I.

HD 76431, however, turned out to be considerably hotter than the other programme stars and the assumption of LTE might be questionable. Therefore a grid of partially line blanketed NLTE model atmospheres (Napiwotzki 1997) was used. These models contain hydrogen and helium. The latest version of the NLTE code by Werner (1986) is used, which employs the Accelerated Lambda Iteration (ALI) technique (Werner & Husfeld 1985; see Werner & Dreizler 1999 for details).

2.1. Effective temperatures and gravities

The fit was executed for all high and low resolution spectra and the results are listed in Table 2. An example fit is reproduced in Fig. 2 to illustrate the excellent quality of the matching of the observations by synthetic spectra. Errors in effective temperatures were estimated conservatively as 5% and we adopted an error of ±0.1 dex for the gravities of all programme stars.

For all stars Strömgren photometry is available, which allowed an independent determination of the effective temperature. We used the program of Moon (1985) as modified by Napiwotzki et al. (1993) to derive the effective temperature and the reddening and compare the photometric temperatures to the spectroscopic ones in Table 2. There is a good agreement between results from low and high resolution spectra and photometry, except for PG 1400+389 for which the two available colour measurements result in rather different $T_{\rm eff}$.

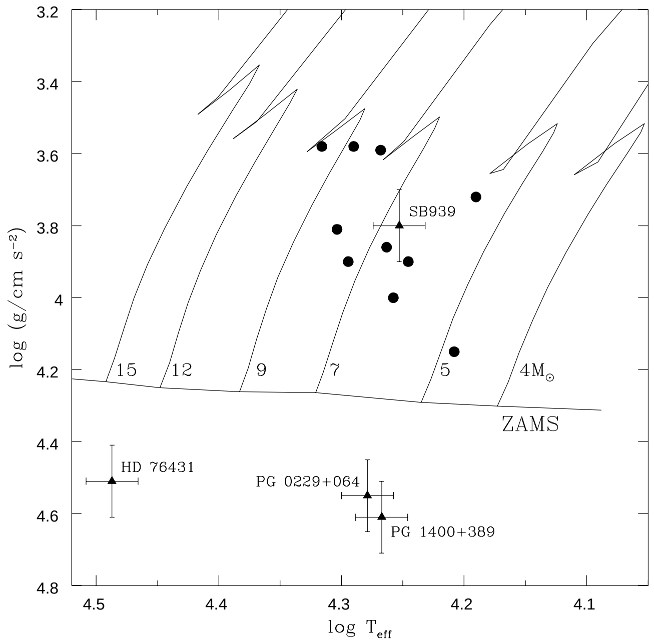

Fig. 1. The positions of the programme stars (triangles with error bars) and that of massive B-type stars from Paper I (filled circles) in the ($T_{\rm eff}$, $\log g$) diagram are compared with evolutionary tracks calculated by Schaller et al. (1992) for main sequence stars. The filled circles are objects with detectable rotation and the triangles for non-rotating objects ($v \sin i < 5$ km s^{-1}).

The parameters used for further analyses were taken from the high resolution spectra, except for PG 1400+389, because the spectral range covered is larger, allowing to use more Balmer and helium lines in the fit procedure. However, in the case of PG 1400+389 the Echelle and the long slit spectrum covered only three Balmer lines. Therefore, we averaged the parameter derived from high and low resolution spectra.

Our results are shown in a ($T_{\rm eff}$, $\log g$) diagram and compared to high latitude main sequence stars (from Paper I) and to evolutionary tracks for main sequence stars (1992, Fig. 1). SB 939 is located in the main sequence band. The other stars, however, lie below the main sequence and therefore cannot be massive stars. Further clues as to the nature of these stars come from the projected rotational velocities and the chemical abundance pattern.

2.2. Helium abundances

An outstanding result of the analysis is the non-solar helium abundance of all programme stars. While in HD 76431 helium is depleted by a factor of 3 with respect

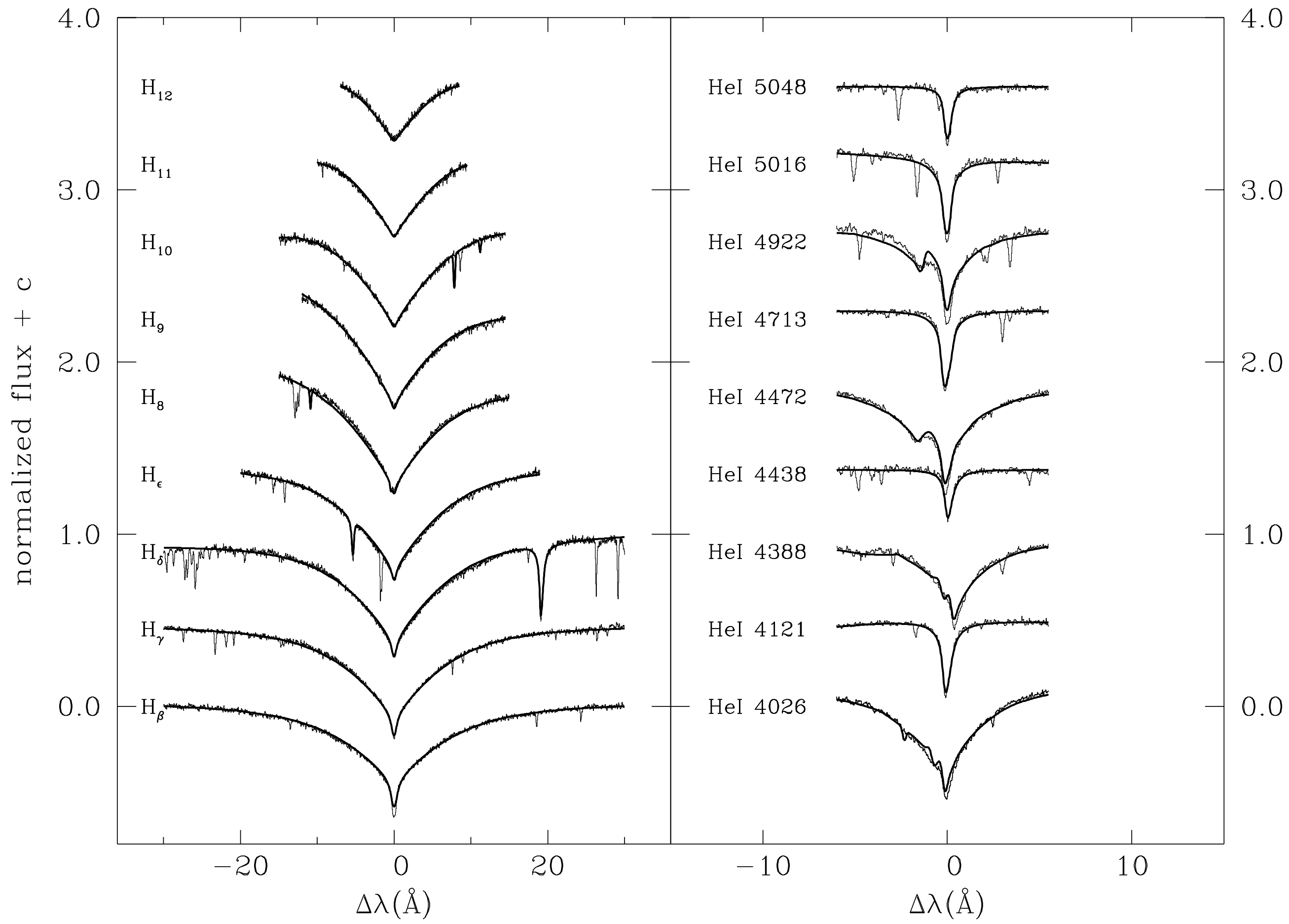

Fig. 2. Fit of the Balmer and helium lines by synthetic spectra for PG 0229+064.

Table 2. Atmospheric parameters and rotational velocities for the programme stars as derived from high and low resolution spectroscopic data and comparison of these data with the effective temperatures calculated from Strömgren photometry. The upper limits of rotational velocities are determined from the Mg II doublet at 4481 Å.

Name	High Resolution				Low Resolution			Photometry	
	$T_{\rm eff}$ (K)	$\log(\frac{g}{\rm cm\,s^{-2}})$	$\log\frac{N({\rm He})}{N({\rm H})}$	$v \sin i$ (km s^{-1})	$T_{\rm eff}$ (K)	$\log(\frac{g}{\rm cm\,s^{-2}})$	$\log\frac{N({\rm He})}{N({\rm H})}$	$T_{\rm eff}$ (K)	$E(b-y)$
PG 0229+064	19 000	4.55	−0.80	<5	19 200	4.51	−0.72	20 200 (1)	0.039
								21 000 (2)	0.036
PG 1400+389	18 200	4.51	−0.60	<5	18 800	4.71	−0.71	20 500 (1)	0.023
								17 100 (3)	0.004
HD 76431	31 000	4.51	−1.51	<5	28 500	4.31	−1.68	30 100 (4)	0.0
SB 939	17 900	3.80	−0.60	<5	–	–	–	18 000 (5)	0.001

Strømgren photometry from: (1) Wesemael et al. (1992); (2) Moehler et al. (1990); (3) Mooney et al. (2000); (4) Kilkenny (1987); (5) Graham J. A. et al. (1973).

to the sun, helium is significantly enriched in the other stars. Figure 3 illustrates the influence of the helium enrichment on the profiles of weak and strong He lines in the case of PG 0229+064, which is only mildly helium rich.

In previous spectral analyses of three of our programme stars (Saffer et al. 1997) based on low resolution spectra, the peculiar helium abundance could not be obtained because the fit procedure was executed assuming a solar helium abundance. This underestimate of the helium abundance also led to considerably higher effective temperatures and gravities for PG 0229+064 and PG 1400+389 than our analyses.

The non-solar helium abundances is another indicator that PG 1400+389 and PG 0229+064 are unlikely to be normal massive B-type stars.

The high helium content of SB 939 was already pointed out by Langhans & Heber (1986) and is confirmed by our analysis. Langhans & Heber (1986) suggested that SB 939

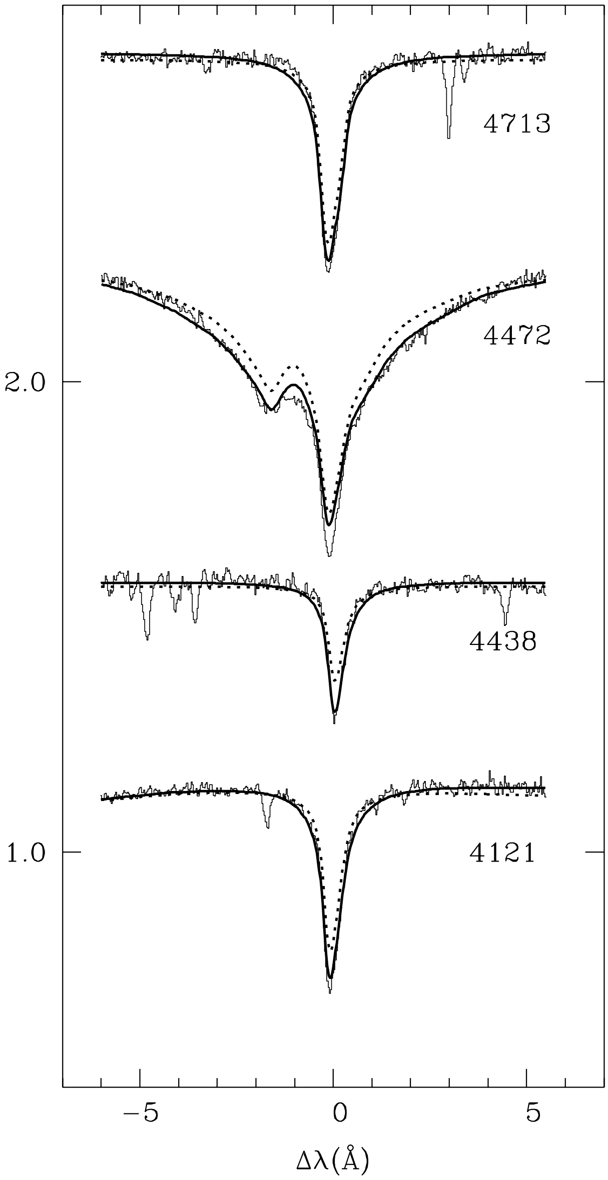

Fig. 3. Comparison of helium lines in the spectrum of PG 0229+064 to synthetic line profiles for helium abundance derived by the fit procedure and for normal helium abundance (dashed).

might belong to the class of intermediate helium stars which are main sequence stars with unusually strong (and sometimes variable) helium lines (for a review see Hunger 1986). They populate a temperature range (22 000 K to 28 000 K) somewhat hotter than SB 939 and are found close to the galactic plane (Drilling 1986). If confirmed, SB 939 would be the first intermediate helium star at high galactic latitudes. But still we cannot exclude that SB 939 belongs to the class of intermediate helium stars.

2.3. Projected rotational velocities

All programme stars display very sharp absorption lines indicating that they are slow rotators unless they are seen pole-on. The components of the Mg II doublet (4481.13/4481.33 Å) are resolved that can be used to estimate the projected rotational velocity. An upper limit of $5\,\mathrm{km\,s^{-1}}$ results for all stars. These low values provide further evidence that the programme stars are unlikely to be main sequence stars.

3. Metal abundances

The equivalent widths were measured employing the nonlinear least-squares Gaussian fitting routines in MIDAS with central wavelength, central intensity and full width at half maximum as adjustable parameters. For metal lines located in direct neighbourhood of Balmer or helium lines an additional Lorentzian function is used to describe the line wings of the latter.

Metal lines of the species C II, C III, N II, N III, O I, O II, Ne I, Ne II, Mg II, Al II, Al III, Si II, Si III, Si IV, P II, P III, S II, S III, Ar II, Ti II, Fe II and Fe III could be identified. The atomic data for the analysis were taken from several tables:

1. CNO from Wiese et al. (1996);
2. Fe from Kurucz (1992) and Ekberg (1993);
3. Ne, Mg, Al, Si, S, P, Ar, Ti from Hirata et al. (1995).

The LTE abundances were derived by using the classical curve–of–growth method and the LINFOR program (version of Lemke, see Paper I). In this case the model atmospheres were generated for the appropriate values of effective temperature, gravity and solar helium and metal abundance with the ATLAS9 program of Kurucz (1992).

Then we calculated curves of growth for the observed metal lines, from which abundances were derived. Blends from different ions were omitted from the analysis. In the final step the abundances were determined from a detailed spectrum synthesis (using LINFOR code described above) of all lines measured before. The results of the LTE abundance analysis and the rms errors for PG 0229+064, PG 1400+389, SB 939, and HD 76431 are shown in Table 3. The number of lines used is given in brackets. Beside the statistical rms errors the uncertainties in $T_{\rm eff}$, $\log g$ and microturbulent velocity (see below) contribute to the error budget.

In order to minimize the systematic errors we have choosen the B-type star τ Sco for HD 76431 and ι Her for the other three targets as comparison stars, since they have similar atmospheric parameters to those of our programme stars. These stars have been analysed by Hambly et al. (1997). We redetermined the LTE abundances of τ Sco and ι Her using the same atomic data, model atmosphere and spectrum synthesis code as the programme stars and took the equivalent widths of unblended lines measured by Hambly et al. (1997).

Our results for ι Her agree to within 0.1 dex with those of Hambly et al. (1997) except for C II (0.12 dex), Si III (0.17 dex), S III (0.21 dex) and Fe III (0.36 dex). In particular our statistical error for Fe III is much lower than that of Hambly et al. (1997).

For τ Sco we also found good agreement with the results of Hambly et al. (1997) except for C II (0.31 dex), C III (0.17 dex), N III (0.13 dex), Al III (0.18 dex), S III (0.17 dex) and Fe III (0.43 dex). The difference for ι Her

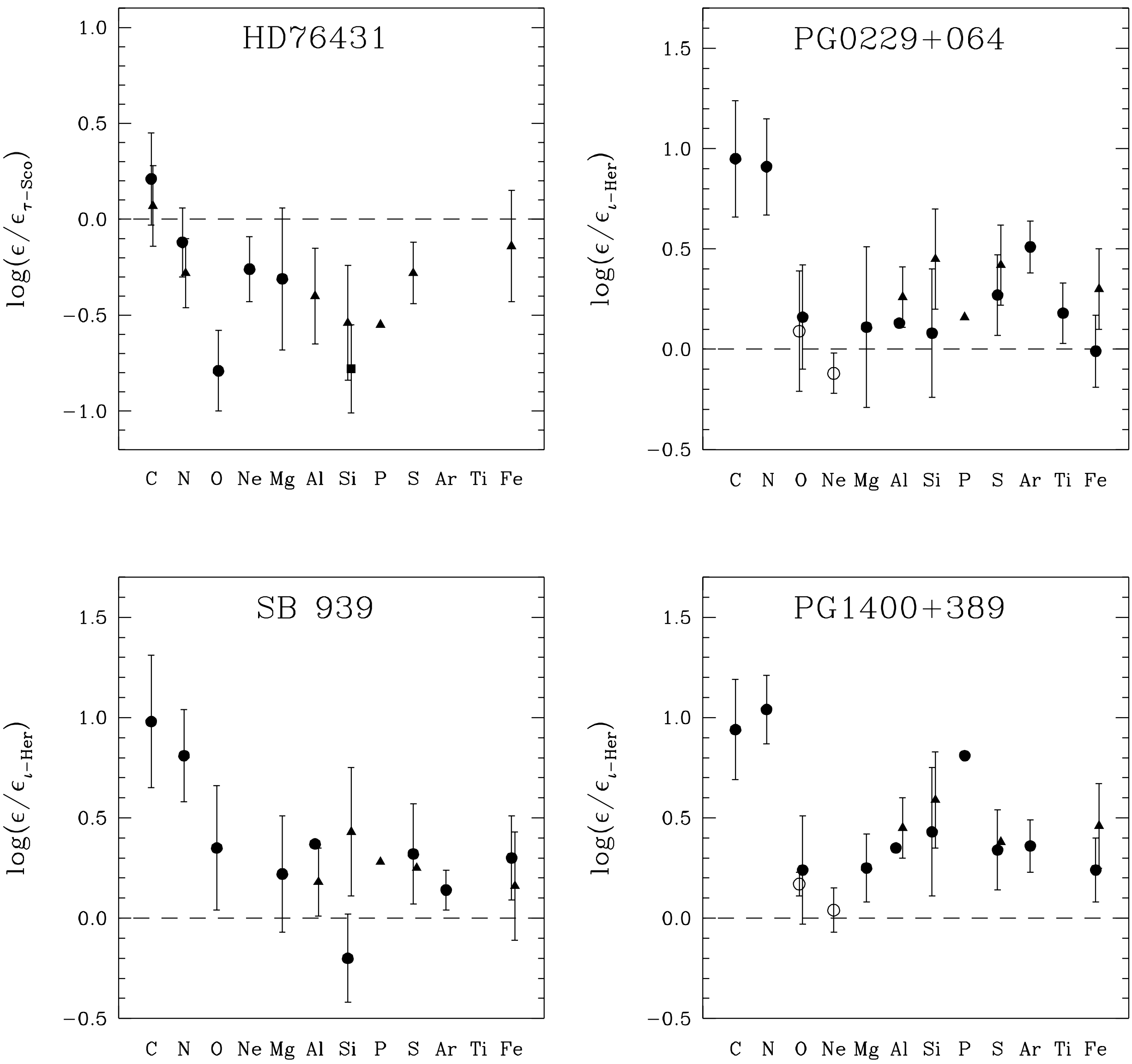

Fig. 4. LTE abundances (relative to τ Sco for HD 76431 and relative to ι Her for the other three stars) and errors of the programme stars. Abundances derived from neutral elements are shown as open circles, from singly ionizied ones as filled circles, from doubly ionizied ones as filled triangles and from triply ionizied ones as filled squares.

and τ Sco between Hambly et al. (1997) and our work can be attributed to different oscillator strengths used (esp. for Fe III) and our neglect of blended lines. Results are given in Tables 3 and 4 and systematic errors are adopted for our programme stars as well. These errors are incorporated in the error bars plotted in Fig. 4. The determination of elemental abundances is interlocked with the microturbulent velocity ξ, that can be derived if a sufficient number of lines of one ion can be measured over a wide range of line strengths. In our programme stars N II and O II lines are most suitable for this purpose since many lines of these ions can be identified. Microturbulent velocities of $\xi = 5$ km s^{-1} were found for PG 0229+064, PG 1400+389 and HD 76431, while a somewhat higher value of $\xi = 8$ km s^{-1} was deduced for SB 939.

In a differential analysis systematic errors should cancel to a large extent. NLTE effects are small for all elements ($\leq$0.1 dex, Kilian 1994) except for Ne I, which is overestimated by LTE calculations (Auer & Mihalas 1973) e.g. by 0.60 dex in the case of ι Her. Correcting our measurements for this NLTE effect the Ne abundances are quite close to that of normal B-type stars (Kilian 1994). Correcting for the NLTE effect on Ne I (0.60 dex, see above) the neon abundance of the three programme stars for which it has been measured is found to be consistent with Kilian's distribution of Ne abundances in normal B-type stars.

The abundances of programme stars with respect to τ Sco for HD 76431 and ι Her for the others are plotted in Fig. 4.

It is well known that considerable variations of metal abundances from star to star occur among normal main sequence B-type stars (e.g. Kilian 1994). This has to be

Table 3. Mean absolute LTE abundances and rms errors for programme stars. The numbers in brackets indicate the number of lines per ion. For ι Her the abundances are determined with the equivalent widths from Hambly et al. (1997). Errors for the programme stars are statistical errors. For ι Her systematic errors due to uncertainties of atmospheric parameters have been determined in this work and are listed in parentheses.

Element	ι Her		PG 0229+064		PG 1400+389		SB 939	
ξ (km s^{-1})	5		5		5		8	
He I	10.78		11.20 ± 0.10	(9)	11.29 ± 0.10	(6)	11.40 ± 0.10	(4)
C II	8.14 ± 0.26	(± 0.21)	9.09 ± 0.21	(26)	9.08 ± 0.14	(17)	9.12 ± 0.25	(4)
N II	7.85 ± 0.18	(± 0.14)	8.76 ± 0.20	(54)	8.89 ± 0.11	(34)	8.66 ± 0.18	(39)
O I			8.81 ± 0.30	(3)	8.96 ± 0.06	(3)	–	
O II	8.72 ± 0.16	(± 0.19)	8.88 ± 0.19	(20)	8.89 ± 0.19	(12)	9.07 ± 0.28	(16)
Ne I			8.44 ± 0.07	(13)	8.60 ± 0.09	(12)	–	
Mg II	7.28 ± 0.20	(± 0.12)	7.39 ± 0.39	(2)	7.53 ± 0.13	(2)	7.50 ± 0.26	(2)
Al II	6.18		6.31	(1)	6.53	(1)	6.55	(1)
Al III	6.31 ± 0.12	(± 0.14)	6.57 ± 0.12	(6)	6.76 ± 0.06	(5)	6.49 ± 0.09	(4)
Si II	6.86 ± 0.50	(± 0.18)	6.94 ± 0.27	(10)	7.29 ± 0.27	(5)	6.66 ± 0.13	(3)
Si III	7.34 ± 0.20	(± 0.21)	7.79 ± 0.13	(6)	7.93 ± 0.11	(5)	7.77 ± 0.24	(4)
P II			–		6.01	(1)	–	
P III	5.53		5.69	(1)	–		5.48	(1)
S II	6.99 ± 0.19	(± 0.05)	7.26 ± 0.22	(49)	7.33 ± 0.19	(35)	7.31 ± 0.24	(25)
S III	6.93 ± 0.32	(± 0.17)	7.35 ± 0.10	(2)	7.31	(1)	7.18	(1)
Ar II	6.64 ± 0.30	(± 0.08)	7.15 ± 0.10	(15)	7.00 ± 0.10	(10)	6.78 ± 0.06	(4)
Ti II	–		5.18 ± 0.15	(2)	–		–	
Fe II	7.18 ± 0.23	(± 0.13)	7.17 ± 0.13	(2)	7.31 ± 0.09	(2)	7.37 ± 0.16	(2)
Fe III	7.33 ± 0.09	(± 0.15)	7.63 ± 0.13	(14)	7.79 ± 0.15	(9)	7.49 ± 0.23	(5)

taken into account when judging whether a measured abundance pattern is peculiar or not (see also Paper I).

3.1. HD 76431

The helium-poor star HD 76431 has C, N and Fe abundances quite similar to τ Sco. Other metals are slightly deficient with respect to τ Sco but well within the range of main sequence B-type stars (except for an oxygen underabundance). If this star were not helium deficient it would be difficult to judge whether its abundance pattern is peculiar or not.

3.2. PG 1400+389 and PG 0229+064

The helium-rich stars PG 1400+389 and PG 0229+064 lie below the main sequence. They display large overabundances of C (0.95 dex) and N (0.9 to 1.05 dex) with respect to ι Her. While O and Ne have abundances similar to ι Her the other metals are somewhat more abundant than in the comparison stars. Such large C and N enhancement is not known to occur in any main sequence B-type star. Therefore it is unlikely that PG 1400+389 and PG 0229+064 are massive B-type stars.

3.3. SB 939

The helium rich star SB 939 lies on the main sequence band and might be an intermediate helium star. The metal abundance pattern (see Fig. 4) is very similar to those of PG 1400+389 and PG 0229+064. In particular, it shares the large enhancement of carbon and nitrogen with the latter. Intermediate helium stars in general display normal C, N and O abundances (Hunger 1986) and therefore it appears unlikely that SB 939 belongs to the class of intermediate helium stars.

4. Evolutionary status

Although our programme stars spectroscopically mimic normal massive B-type stars when studied at low spectral resolution, the high resolution spectral analysis presented above revealed mounting evidence that the programme stars cannot be young massive stars.

Low-mass stars can reach the high temperatures in question during their evolution in the horizontal branch, post-extreme horizontal branch and post-AGB phase (see Heber 1992 for a review). We therefore compare the positions of the four stars in the ($T_{\rm eff}$, $\log g$) diagram to the

Table 4. Mean absolute LTE abundances and rms errors for HD 76431. The numbers in brackets indicate the number of lines per ion. For τ Sco the abundances are determined with the equivalent widths from Hambly et al. (1997). Errors for the programme stars are statistical errors. For τ Sco systematic errors due to uncertainties of atmospheric parameters have been determined in this work and are listed in parentheses.

Element	τ Sco		HD 76431	
ξ (km s^{-1})	6		5	
He I	11.10		10.49 ± 0.10	(7)
C II	8.28		8.49 ± 0.09	(15)
C III	8.48 ± 0.22	(± 0.14)	8.55 ± 0.16	(22)
N II	8.20 ± 0.19	(± 0.07)	8.08 ± 0.17	(65)
N III	8.46 ± 0.18	(± 0.16)	8.18 ± 0.09	(10)
O II	8.60 ± 0.17	(± 0.10)	7.81 ± 0.19	(44)
Ne II			8.30 ± 0.17	(4)
Mg II	7.53		7.22 ± 0.36	(2)
Al III	6.39 ± 0.03	(± 0.08)	5.99 ± 0.24	(5)
Si III	7.49 ± 0.74	(± 0.15)	6.95 ± 0.26	(7)
Si IV	7.50 ± 0.12	(± 0.17)	6.72 ± 0.15	(5)
P III	5.59		5.04	(1)
S III	6.87 ± 0.18	(± 0.14)	6.59 ± 0.08	(6)
Fe III	7.36 ± 0.37	(± 0.10)	7.22 ± 0.27	(16)

predictions of evolutionary calculations for these phases of evolution (see Fig. 5). The gravities of all four stars are too high to be consistent with post-AGB evolution. PG 0229+064 and PG 1400+389 lie close to the horizontal branch. However, their abundance anomalies are unusual for horizontal branch stars which are mostly helium-deficient instead of helium-rich (as observed). There is general consensus that the abundance patterns of horizontal branch stars are caused by diffusion processes, which lead to the observed underabundances of helium due to gravitational settling. Therefore the identification of PG 0229+064 and PG 1400+389 as horizontal branch stars may be premature. We may speculate that the C and N enrichment may indicate that dredge-up of material processed by the CN cycle (N) and helium burning (C) may have occurred. This conjecture is corroborated by the observed helium enrichment. This requires deep mixing into the helium core in order to dredge up carbon which is unlikely to occur in horizontal branch stars.

HD 76431 and SB 939 lie above the horizontal branch. The low helium abundance of HD 76431 indicates that diffusion processes are going on in its atmosphere as would be expected for a star evolving from the horizontal branch. Comparing its position to evolutionary tracks of Dorman et al. (1993, see Fig. 5) we conclude that HD 76431 is in the post-EHB stage and evolves towards the white dwarf cooling sequence.

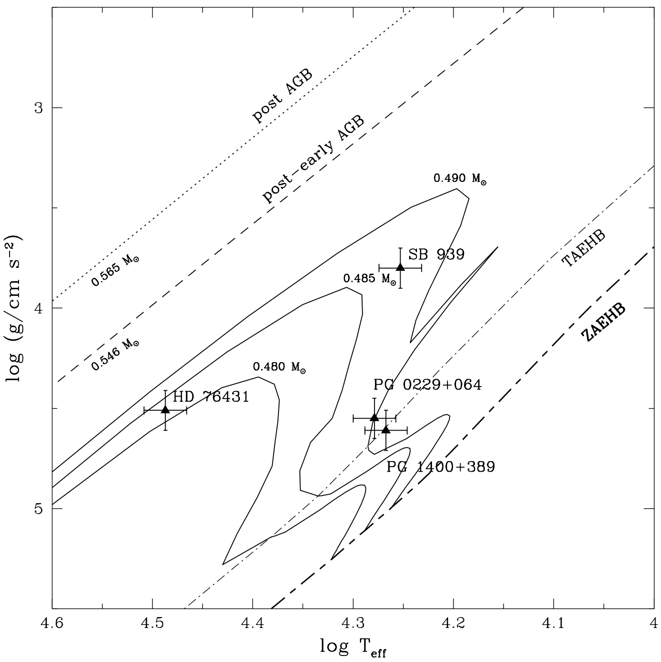

Fig. 5. Comparison of the helium rich stars PG 0229+064, PG 1400+389, SB 939 and the helium poor star HD 76431 in the (T_{eff}, $\log g$) diagram, to evolutionary EHB-tracks of Dorman et al. (1993), post-early AGB + post-AGB tracks of Schönberner (1983).

The He, C and N enrichment of SB 939 again calls for a dredge-up mechanism which is difficult to envisage, as discussed above already.

Diffusion processes in the atmospheres of SB 939, PG 0229+064 and PG 1400+389 must be somewhat different from those in normal HB and post-HB stars. Physical processes that could modify diffusion are e.g. mass loss and magnetic fields. Therefore it would be useful to search for the presence of magnetic fields and stellar winds in these stars.

5. Kinematics

A study of their kinematics may give additional clues as to the nature of these stars. Proper motions for our programme stars have become available recently (see Table 5) through the Hipparcos/Tycho catalogs (Perryman et al. 1997; Høg et al. 1998) and the work by Thejll et al. (1997). Space motions can be derived when radial velocities and distance are known. These quantities can be determined spectroscopically.

5.1. Radial velocities and distances

Radial velocities were derived from the lineshift of metal lines and corrected to heliocentric values. Results are listed in Table 6. The error of the velocities estimated from the scatter of the velocities derived from individual metal lines is about 2–5 km s^{-1}.

Table 5. Data of proper motion. For the programme stars the position angle is counted positive east of north.

Name	μ (mas/y)	Position angle °	Reference
PG 0229+064	18.0 ± 3.3	84 ± 16	1
PG 1400+389	6.9 ± 3.8	223 ± 58	1
HD 76431	38.0 ± 8.0	233 ± 15	2
SB 939	18.7 ± 15.4	204 ± 50	3

References: (1) Thejll et al. (1997); (2) Perryman et al. (1997); (3) Høg et al. (1998).

Table 6. Radial velocities and spectroscopic distances.

Name	$v_{\rm rad}$ km s^{-1}	d pc
PG 0229+064	$(8 \pm 2)^{\star}$, $(8 \pm 3)^{\star\star}$	740 ± 117
PG 1400+389	34 ± 2	810 ± 134
HD 76431	47 ± 2	370 ± 61
SB 939	-25 ± 4	860 ± 134

* Obtained from KECK high resolution spectrum;
** Obtained from FOCES high resolution spectrum.

The distance has been calculated from mass, effective temperature, gravity and the dereddened apparent magnitude of the stars:

$$d = 1.11\sqrt{\frac{M_{\star}F_V}{g} \times 10^{0.4V_0}} \text{ [kpc]}$$

where $M_{\star}$ is the stellar mass in $M_{\odot}$, g is the gravity in cm s^{-2}, F_V is the model atmosphere flux at the stellar surface in units of 10^8 erg cm^{-2} s^{-1} Å^{-1} and V_0 is the dereddened apparent visual magnitude. $M_{\star} = 0.5\,M_{\odot}$ has been adopted in accordance with the prediction of evolutionary models.

For HD 76431 a trigonometric parallax has been measured by Hipparcos: $\pi = 3.55 \pm 1.83$ mas resulting in a distance of 280^{+280}_{-95} pc in good agreement with the spectroscopic distance (370 ± 61 pc).

5.2. Galactic orbits and population membership

In order to find out to which stellar population the stars belong we calculated galactic orbits backwards in time for 10 Gyrs using the program ORBIT6 developed by Odenkirchen & Brosche (1992). This numerical code calculates the orbit of a test body in the galactic potential of Allen & Santillan (1991). A detailed description of the method is given by Altmann & de Boer (2000). The complete set of cylindrical coordinates is integrated and positions and velocities are calculated in equidistant time steps. The input for this program version are equatorial coordinates, distance d from the sun, heliocentric radial velocities and observed absolute proper motions. Meridional projections of the orbits are shown in Fig. 6.

Table 7. Parameters of galactic orbits $z_{\rm max}$ is the maximum distance from the galactic plane, e is the eccentricity of the orbit and Θ is the orbital velocity.

Name	$z_{\rm max}$ [kpc]	e	Θ [km s^{-1}]
PG 0229+064	0.86	0.18	211
PG 1400+389	1.29	0.02	213
HD 76431	0.47	0.25	206
SB 939	1.39	0.31	200

The maximum heights above the galactic plane, the eccentricities and orbital velocities are summarized in Table 7. These data are consistent with HBB stars analysed by Altmann & de Boer (2000). The orbital velocities are slightly lower than that of $\Theta_{\rm LSR}$ (220 km s^{-1}) and the orbits are slightly eccentric. The small maximum heights above the plane indicate that the stars belong to an old disk population.

6. Conclusions

We have carried out differential spectral analyses of four apparently normal B-type stars. PG 0229+064, PG 1400+389, HD 76431 and SB 939 are found to be sharp lined. This indicates that the projected rotational velocity is low ($v \sin i < 5$ km s^{-1}). The former three lie below the ZAMS in the ($T_{\rm eff}$, $\log g$) diagram. Peculiar helium abundances are found, PG 0229+064, PG 1400+389 and SB 939 being helium rich, HD 76431 being helium poor due to diffusion. Therefore we conclude that these four stars cannot be young massive B-type stars but must be evolved low-mass B-type stars.

While PG 0229+064 and PG 1400+389 could be explained as horizontal branch stars from their position in the ($T_{\rm eff}$, $\log g$) diagram, HD 76431 and SB 939 must already have evolved beyond the horizontal branch. The atmospheric abundance patterns of stars in these phases of evolution are known to be dominated by diffusion processes, the clear-cut indicator being a typical helium deficiency. Such an helium underabundance is indeed observed for HD 76431, indicating that it has evolved from the extreme horizontal branch. The other stars are helium rich. The enrichment in helium, carbon and nitrogen can be explained either by deep mixing of nuclearly processed material to the surface or by diffusion processes modified by magnetic fields and/or stellar winds. A search for magnetic fields and stellar winds is proposed.

Based on proper motion and radial velocity measurements and spectroscopic distances the galactic orbits of the stars have been calculated backwards in time. An analysis of the orbits indicates that the stars belong to an old disk population.

Acknowledgements. M.R. and H.E. gratefully acknowledge financial support by the DFG (grant He1356/27-1). We thank

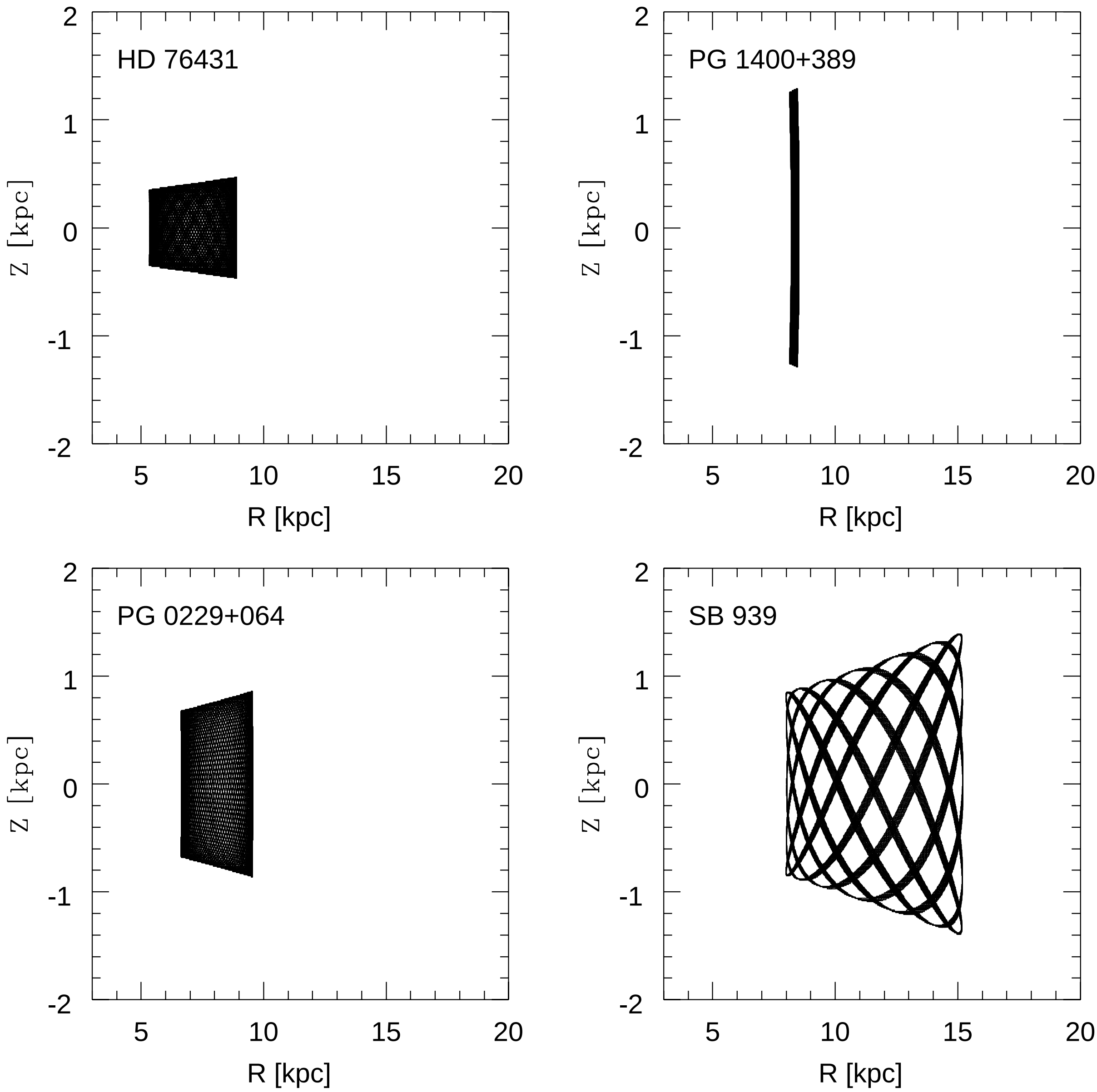

Fig. 6. Meridional projections of the galactic orbits during the last 10 Gyrs.

Neil Reid who provided us with the Keck observations and Thomas Rauch who obtained the DSAZ TWIN spectra for us.

References

Allen, C., & Santillan, A. 1991, Rev. Mex. A&A, 22, 255

Altmann, M., & de Boer, K. S. 2000, A&A, 353, 135

Auer, L. H., & Mihalas, D. 1973, ApJ, 184, 151

Dorman, B., Rood, R. T., & O'Connell, R. W. 1993, ApJ, 419, 596

Drilling, J. S. 1986, in Hydrogen Deficient stars and Related Objects, ed. K. Hunger, D. Schönberner, & N. K. Rao, ASSL 128 (Reidel), 9

Ekberg, J. O. 1993, A&AS, 101, 1

Graham, J. A., & Slettebak, A. 1973, AJ, 78, 295

Hambly, N., Keenan, F. P., Dufton, P. L., et al. 1996, ApJ, 466, 1018

Hambly, N., Rolleston, W. R. J., Keenan, F. P., Dufton, P. L., & Saffer, R. A. 1997, ApJS, 111, 419

Heber, U. 1992, Proceedings of the Kiel/CCP7 workshop on Atmospheres of Early-Type Stars, ed. U. Heber, & C. S. Jeffery (Springer), Lect. Notes in Phys., 401, 233

Heber, U., Moehler, S., & Groote, D. 1995, A&A, 303, L33

Heber, U., Moehler, S., Schmidt, J. H. K., et al. 1997, in The Third Conference on Faint Blue Stars, ed. A. G. Davis Philip, J. W. Liebert, & R. Saffer (Schenectady, L. Davis press), 87

Hirata, R., & Horaguchi, T. 1995, Atomic Spectral Line List, Department of Astronomy (Kyoto University and National Science Museum, Tokyo)

Høg, E., Kuzmin, A., Bastian, U., et al. 1998, A&A, 335, 65

Hunger, K. 1986, in Hydrogen Deficient stars and Related Objects, ed. K. Hunger, D. Schönberner, & N. K. Rao, ASSL 128 (Reidel), 261

Keenan, F. P. 1992, QJRAS, 33, 32

Kilian, J. 1994, A&A, 282, 867

Kilkenny, D. 1987, MNRAS, 228, 713
Kurucz, R. 1992, in The Stellar Population of Galaxies, ed. B. Barbuy, & A. Renzini (Kluwer, Dordrecht), IAU Symp., 149, 225
Langhans, G., Heber, U. 1986, in Hydrogen Deficient stars and Related Objects, ed. K. Hunger, D. Schönberner, & N. K. Rao, ASSL 128 (Reidel), 309
Moehler, S., Richtler, T., de Boer, K. S., Dettmar, R. J., & Heber, U. 1990, A&AS, 86, 53
Moehler, S., Heber, U., & Dreizler, S. 1994, A&A, 282, 29
Moon, T. T. 1985, Comm. Univ. London Obs., 78
Mooney, C. J., Rolleston, W. R. J., Keenan, F. P., Pinfield, D. J., & Pollaco, D. L. 2000, A&A, 357, 553
Napiwotzki, R., Schönberner, D., & Wenske, V. 1993, A&A, 268, 653
Napiwotzki, R. 1997, A&A, 322, 256
Odenkirchen, M., & Brosche, P. 1992, Astron. Nachr., 313, 69
Perryman, M. A. C., Lindgren, L., Kovalevsky, J., Hog, E., & Bastian, U. 1997, A&A, 323, L49
Ramspeck, M., Heber, U., & Moehler, S. 2001, A&A, submitted
Saffer, R. A., Keenan, F. P., Hambly, N. C., Dufton, P. L., & Liebert, J. 1997, ApJ, 491, 172
Schaller, G., Schaerer, D., Meynet, G., & Maeder, A. 1992, A&AS, 96, 269
Schmidt, J. H. K., de Boer, K. S., Heber, U., & Moehler, S. 1996, A&A, 306, L33
Schönberner, D. 1983, ApJ, 272, 708
Thejll, P., Flynn, C., Williamson, R., & Saffer, R. 1997, A&A, 317, 689
Tobin, W. 1987, in The 2nd Conference on Faint Blue Stars, IAU Coll. 95, ed. A. G. D. Philip, D. S. Hayes, & J. W. Liebert (L. Davis press), 149
Werner, K., & Husfeld, D. 1985, A&A, 148, 417
Werner, K. 1986, A&A, 161, 177
Werner, K., & Dreizler, S. 1999, J. Comp. Appl. Math. (Elsevier), 109, 65
Wesemael, F., Fontaine, G., Bergeron, P., Lamontagne, R., & Green, R. F. 1992, AJ, 104, 203
Wiese, W. L., Fuhr, J. R., & Deters, T. M. 1996, Atomic Transitions Probalbilities of Carbon, Nitrogen and Oxygen (National Institute of Standards and Technology, Gauthersburg, Maryland)